Computational and Systems Biology
Physics of Living Systems

ElegansBot: Development of equation of motion deciphering locomotion including omega turns of *Caenorhabditis elegans*

Taegon Chung, Iksoo Chang, Sangyeol Kim

Department of Brain Sciences, Daegu Gyeongbuk Institute of Science and Technology, Korea

https://en.wikipedia.org/wiki/Open_access
Copyright information

Reviewed Preprint

Revised by authors after peer review.

About eLife's process

Reviewed preprint version 2
March 27, 2024 (this version)

Reviewed preprint version 1
December 19, 2023

Posted to preprint server
September 27, 2023

Sent for peer review
September 11, 2023

Abstract

Locomotion is a fundamental behavior of *Caenorhabditis elegans* (*C. elegans*). Previous works on kinetic simulations of animals helped researchers understand the physical mechanisms of locomotion and the muscle-controlling principles of neuronal circuits as an actuator part. It has yet to be understood how *C. elegans* utilizes the frictional forces caused by the tension of its muscles to perform sequenced locomotive behaviors. Here, we present a two-dimensional rigid body chain model for the locomotion of *C. elegans* by developing Newtonian equations of motion for each body segment of *C. elegans*. Having accounted for friction-coefficients of the surrounding environment, elastic constants of *C. elegans*, and its kymogram from experiments, our kinetic model (ElegansBot) reproduced various locomotion of *C. elegans* such as, but not limited to, forward-backward-(omega turn)-forward locomotion constituting escaping behavior and delta-turn navigation. Additionally, ElegansBot precisely quantified the forces acting on each body segment of *C. elegans* to allow investigation of the force distribution. This model will facilitate our understanding of the detailed mechanism of various locomotive behaviors at any given friction-coefficients of the surrounding environment. Furthermore, as the model ensures the performance of realistic behavior, it can be used to research actuator-controller interaction between muscles and neuronal circuits.

eLife assessment

This **useful** study introduces a simple mechanical model of C. elegans locomotion that captures aspects of the worm's behavioral repertoire beyond forward crawling. While the kinetic model (ElegansBot) provides a compromise and starting point to help understand the mechanical components of C. elegans behavior, the claim that this work improves on extant mechanical models is **incomplete**, including modeling a 3-dimensional turning behavior with a 2-dimensional model without sufficient justification. In addition, the results of the application of the model to previously unstudied behaviors are primarily qualitative and do not produce new predictions.

Introduction

With only a few hundred neurons, *Caenorhabditis Elegans*(*C. elegans*) performs various behaviors such as locomotion, sleeping, reproduction, and hunting (Hall & Altun, 2008). The connectome structure among 302 neurons and 165 somatic cells of *C. elegans* was discovered by pioneering works (Cook et al., 2019; White et al., 1986). *C. elegans* is a cost-efficient and widely-used model in neuronal research. Its small body size and minimal nutritional requirements contribute to its cost efficiency. The organism matures in a shorter period, about three days, compared to other model animals such as fruit flies or mice. Its transparent body allows for easy microscopic observation of its internal structures or artificially expressed green fluorescent proteins. Moreover, due to the hermaphroditic nature of *C. elegans*, offspring mostly share the same genotype as the parent, which simplifies the multiplication of the worm population for research purposes (Hall & Altun, 2008).

C. elegans bends its body with a sinusoidal wave pattern when moving forward or backward. The driving force for this movement comes from the difference between perpendicular and parallel frictional forces, which it experienced from a surrounding environment. This thrust force pushes the worm along the ground surface with which the worm contacts(Boyle, 2009; Boyle et al., 2012; Hu et al., 2009; Niebur & Erdös, 1991). Even if a worm has a sinusoidal modulation generated inside it, it has difficulties in forward and backward locomotion if it does not feel the difference in frictional forces from its surroundings.

Mechanical simulators of rod-shaped animals such as *C. elegans* (Boyle et al., 2012; Niebur & Erdös, 1991), fish (Ekeberg, 1993), and snakes (Hu et al., 2009) have been used in various studies. These simulators demonstrate how the activities of muscle cells are represented as behavioral phenotypes, which are determined by signals from a neuronal circuit simulator (Boyle et al., 2012; Ekeberg, 1993; Niebur & Erdös, 1991). They also show how muscle cells return proprioceptive signals back to the neuronal circuit simulator and how animals intentionally distribute body weight for locomotion patterns (Hu et al., 2009). Similarly, the kinematic simulator of fish(Ekeberg, 1993), which has a locomotion pattern in that the animal mostly undulates in a particular direction, was used with a neuronal network simulator to model the undulation of swimming behavior. This combination of kinematic simulator and neuronal network simulator was also used to model how the locomotion pattern changes due to a surrounding environment(Boyle et al., 2012) and how the central pattern generator arises from a few cells(Boyle et al., 2012; Izquierdo & Beer, 2018).

Even though there were studies on kinematic simulation of rod-shaped animals (Boyle et al., 2012; Ekeberg, 1993; Hu et al., 2009), to our best knowledge, there was no kinetic model that reproduces complex locomotion behavior of *C. elegans*, which includes all of the various modes of locomotion of *C. elegans* such as forward locomotion, backward locomotion, and turn from experimental observations. Instead, muscle cell activities from Ansatz (Hu et al., 2009), a hypothesis of the solution, or signals from a neuronal circuit simulator (Boyle et al., 2012; Ekeberg, 1993) were applied to the kinematic simulators. A simulator should have an operational structure that imitates physical quantities from an experiment to reproduce the motion of *C. elegans* of the experiment. However, until now, no kinetic simulation has such a structure. If there is a simulator that reproduces the motion of individual experiments, analysis of the kinetics of motion of specific experiments, which provides information on the individual force that exerts on each body part of the animal, will be enabled. Also, as the kinetic simulation reproduces the motion of *C. elegans*, the behavioral phenotype that emerged from the muscle activity of neuronal circuit simulation will be more credible.

We built a Newtonian-mechanics 2-dimensional rigid body chain model of *C. elegans* to reproduce its locomotion. We incorporated its body angle, related to the contraction of the body wall muscle of *C. elegans*, into the primary operating principle of our kinetic model so that the model simulates measurable physical quantities of *C. elegans* from its experimental video. The model includes a chain of multiple rod rigid bodies, a damped torsional spring between the rigid bodies, and a control angle, which is the dynamic baseline angle from the value of the kymogram of a physical experiment. We formulated Newtonian equations of translational and rotational motion of the rigid body model and computed the numerical solution of the equations by numerical integration using semi-implicit Euler method. As a result, we were able to demonstrate trajectories and kinetics of the general locomotion of *C. elegans*, such as crawling, swimming (Vidal-Gadea et al., 2011), omega-turn, and delta-turn (Broekmans et al., 2016).

Results

Newton's equation of motion for locomotion of *Caenorhabditis elegans:* How does EleganSBot work?

We introduce the simple chain model of *C. elegans*' body. *C. elegans* has an elongated body along the head-to-tail axis. Thus, the worm's body can be approximated as a midline extended along the anterial-posterial axis in the xy-coordinate plane (**Fig. 1A**). Let M (=2 μg, details in "Worm's mass, actuator elasticity coefficient, and damping coefficient" of Supplementary Information) be the mass and L (=1 mm) be the length of the worm. Midline was approximated as n (=25) straight rods, whose ends are connected to the ends of neighboring rods (**Fig. 1A**). The mass, length, and moment of inertia of each rod is $m= M/n$, $2r = L/n$, and $I=mr^2/3$ respectively. When numbering the rods in order, with the rod at the end of the head being labeled as "1-rod" and the rod at the end of the tail being labeled as "n-rod", let us designate the i-th rod as "i-rod". The point where i-rod and (i+1)-rod meets is "i-joint".

The motion of the worm corresponds to the motion of all the rods. To describe the motion of each rod (i-rod), we need to determine the displacement vector (d), velocity vector (V_i), the angle measured counterclockwise from the positive x-axis to the tangential direction of the rod (s_i) (**Fig. 1B**), and angular velocity (ω_i) of i-rod at a given time t. However, the minimum information required to describe the motion of all rods includes the displacement vector ($\mathbf{d_c}$) and velocity vector ($\mathbf{V_c}$) of the worm's center of mass, s_i and ω_i for each rod (Details in "Minimum information required to describe the motion of each rod" of Supplementary Information, Fig. S1).

Value of time-dependent variable such as $\mathbf{d_c}$, $\mathbf{V_c}$, s_i, and ω_i at given time, t will be expressed as $*^{(t)}$. When initial values, $\mathbf{d}_c^{(0)}$, $\mathbf{v}_c^{(0)}$, $s_i^{(0)}$, and $\omega_i^{(0)}$ are given, the Newtonian equation of motion for acceleration, $\mathbf{a}_c$ and angular acceleration, $\{\alpha_i\}_{i\in\{1,\cdots,n\}}$ must be acquired and numerically integrated twice to find $\mathbf{d}_c^{(t)}$, $\mathbf{v}_c^{(t)}$, $s_i^{(t)}$, and $\omega_i^{(t)}$ at a given time, t. To obtain the Newtonian equations of motion, we must find every force and torque acting on each rod. There are frictional force, muscle force, and joint force among types of forces acting on the rod, and there are frictional torque, muscle torque, and joint torque among types of torques whose descriptions are as follows.

The only external force acting on the worm is frictional force from a ground surface such as an agar plate or water. The frictional force is an anisotropic Stokes frictional force, with a magnitude proportional to the speed and assumed different friction coefficients in perpendicular and parallel directions (Boyle et al., 2012), which guarantees that linearity in velocity is preserved in frictional force as well (Details in "Preservation of linearity in friction" of Supplementary Information). Because of this preservation of linearity, the frictional forces of translational motion

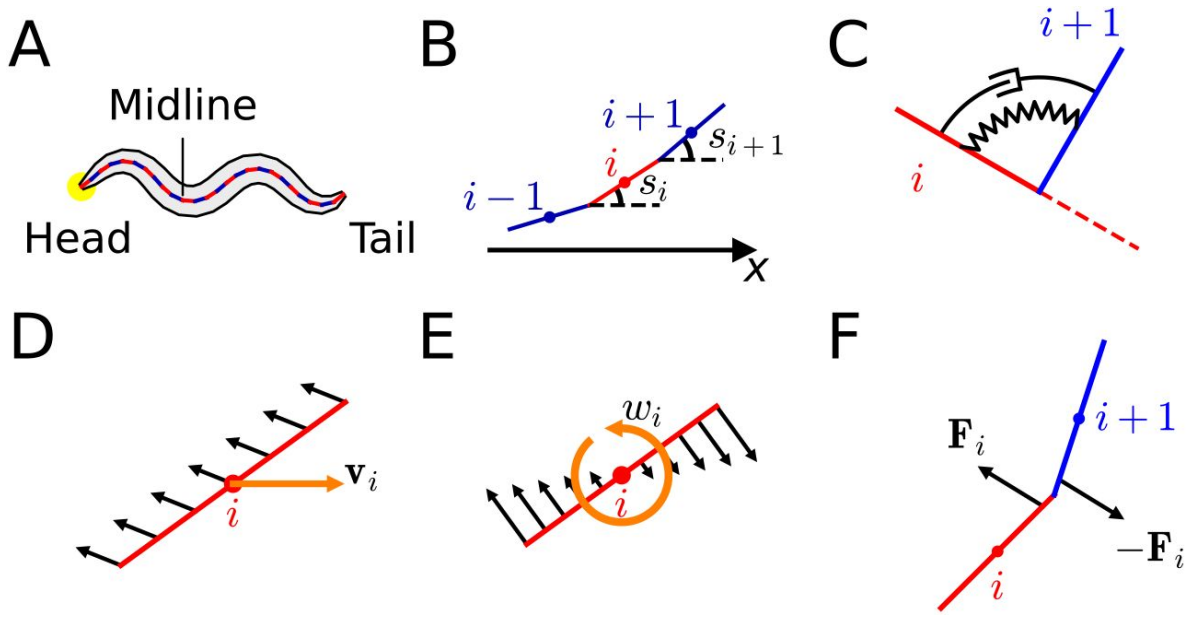

Figure 1.

Components of EleganSBot.

(A) Chain model for *C. elegans* body. (B) Rods in chain model. (C) i-actuator, which is a damped torsional spring. (D) Frictional force (black arrow) due to the translation motion of a rod. (E) Frictional force (black arrow) due to the rotational motion of a rod. (F) Joint force (black arrows) acting on i-rod and (i+1)-rod.

(**Fig. 1D**) and rotational motion (**Fig. 1E**) can be calculated separately and added together to find total frictional force and torque. Previously known values of the friction coefficients in perpendicular and parallel directions are used (Boyle et al., 2012).

Let the perpendicular and parallel friction coefficients be $b_\perp$ and $b_\parallel$ for a straightened worm, respectively. Each rod experiences 1/n of the frictional force the worm gets. Thus, the perpendicular and parallel friction coefficients of each rod are $b_\perp/n$, $b_\parallel/n$, respectively. The ratio of perpendicular friction coefficient to parallel friction coefficient ($b_\perp/b_\parallel$) is 40 in agar plate and 1.5 in water (Boyle, 2009; Boyle et al., 2012). This ratio is an important determining factor in whether the locomotion would be crawling or swimming(Boyle et al., 2012). The total frictional force that i-rod receives is $\mathbf{F}_{b,i} = -\frac{b_\parallel}{n}(\mathbf{v}_i \cdot \hat{\mathbf{r}}_i)\hat{\mathbf{r}}_i - \frac{b_\perp}{n}(\mathbf{v}_i \cdot \hat{\mathbf{N}}_i)\hat{\mathbf{N}}_i$ ("·": dot product of vectors, $\hat{\mathbf{r}}_i \equiv [\cos(s_i) \quad \sin(s_i)]^\mathrm{T}$: unit vector parallel to i-rod $\hat{\mathbf{N}}_i \equiv [-\sin(s_i) \quad \cos(s_i)]^\mathrm{T}$: unit vector perpendicular to i-rod), and the total frictional torque that i-rod receives is $\tau_{b,i} = -\frac{1}{3}\frac{b_\perp}{n}r^2\omega_i$ (positive or negative values are for torque pointing away from or into the paper plane, respectively.) (The proof is in "Frictional torque by rotational motion" of Supplementary Information).

Mature hermaphrodite *C. elegans* has four muscle strands at the left dorsal, right dorsal, left ventral, and right ventral part of the body, and each muscle strand has 24, 24, 23, and 24 muscle cells, respectively (White et al., 1986). Muscle cells at similar positions on the anterior-posterior axis have an activity pattern in that muscles on one side (either dorsal or ventral) cooperate, and those on the opposite side have alternative activities. (Hall & Altun, 2008).

Therefore, we modeled a group of about four muscle cells, which are left dorsal, right dorsal, left ventral, and right ventral, at the same position on the anterior-posterior axis as one actuator (**Fig. 1C**) so that there is a total of 24 ($\simeq (24 + 24 + 23 + 24)/4$) actuators in the worm. On i-joint of the chain, there is an actuator labeled as i-actuator. As the number of actuators is 24, we set the number of rod(n) as 25, which is one more than the number of actuators. The actuator was modeled as a damped torsional spring due to the viscoelastic characteristics of muscle(Boyle et al., 2012; Hill, 1937). If the dorsal muscles of i-actuator contract more than the ventral muscles, i-actuator will bend to the dorsal direction and vice versa. To express this phenomenon by an equation, we defined the torque that i-actuator exerts on i-rod as $\tau_i = \tau_{k,i} + \tau_{c,i}$ that the elastic term is $\tau_{k,i} = k(\theta_i - \theta_{\mathrm{ctrl},i})$ and the damping term is $\tau_{c,i} = c(\omega_{i+1} - \omega_i)$ where $\theta_{ctrl,i}$ is control angle, $\theta_i = s_{i+1} - s_i$, and k and c are the elasticity and damping coefficients of an actuator, respectively.

Control angle ($\theta_{ctrl,i}$) is a variable inside the elastic part of the muscle torque ($\tau_{k,i}$), to which $\tau_{k,i}$ drives θ_i close. Also, control angle ($\theta_{ctrl,i}$), which can be expressed by a heatmap (**Fig. 2A, 2C**, **3A, 3B**), is an input value based on experimental data, a numerical model, or a neuronal network model. $\tau_{c,i}$ represents the damping effect of muscle cells and somatic cells near i-actuator. The elasticity coefficient (κ) and damping coefficient (c) of an actuator were induced from previously known values(Boyle et al., 2012) (Details in "Worm's mass, actuator elasticity coefficient, and damping coefficient" of Supplementary Information).

By assuming that i-rod receives torque (τ_i) from i-actuator, and (i+1)-rod receives torque ($-\tau_i$), we can depict the bending that arises from the differential contraction of dorsal and ventral muscles in i-actuator. The total muscle torque that i-rod receives from damped torsional springs on both ends is $\tau_{ck,i} = \tau_i - \tau_{i-1}$. The total muscle force ($\mathbf{F}_{c\kappa,i}$) that i-rod receives from both of its ends is as follows (Details in "Proof of muscle force" of Supplementary Information, Fig. S2).

$$\mathbf{F}_{c\kappa,i} = \sum_{j=-1}^{0} \frac{(-1)^{j-1}\tau_{i+j}\sin\frac{\theta_{i+j}}{2}}{r\cos^2\frac{\theta_{i+j}}{2}} \begin{bmatrix} \cos\left(\frac{s_{i+j} + s_{i+j+1}}{2}\right) \\ \sin\left(\frac{s_{i+j} + s_{i+j+1}}{2}\right) \end{bmatrix}$$

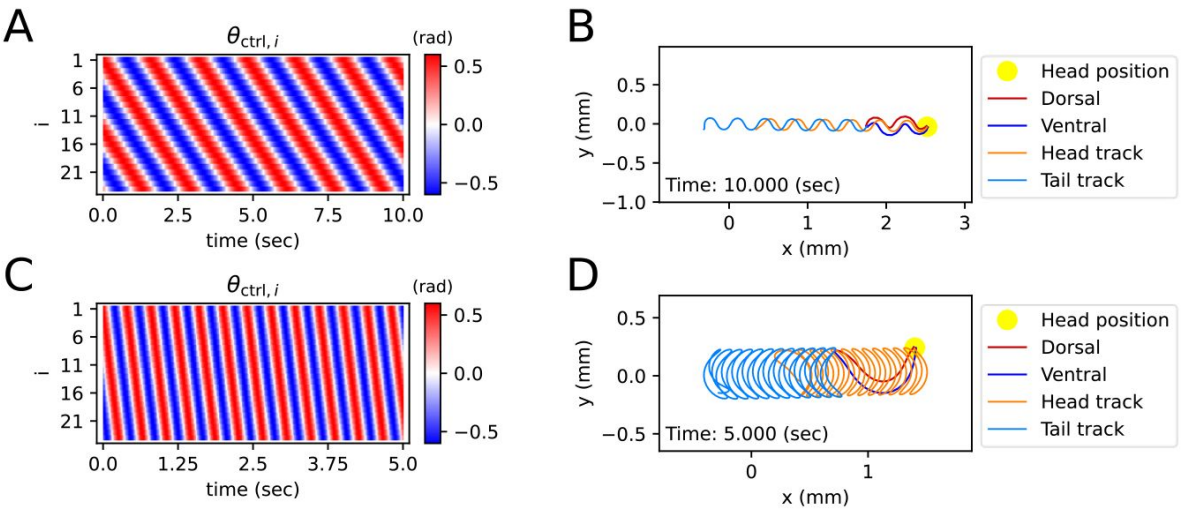

Figure 2.

Simulated locomotion from a sine kymogram.

(A) Crawling kymogram. Kymogram indicates the angle of i-joint which is located between i-rod and (i+1)-rod. Red and blue color mean i-joint bend in the dorsal and ventral directions, respectively. (B) Crawling trajectory. The yellow circle indicates the position of the worm's head. The Orange and sky-blue lines show the worm's head and tail trajectories, respectively. (C) Swimming kymogram. (D) Swimming trajectory

Two neighboring rods (i-rod and (i+1)-rod) are connected at i-joint. Therefore, when a force is applied to i-rod, (i+1)-rod also receives distributed force (**Fig. 1F**) which we name as "joint force". The joint force that (i+1)-rod exerts on i-rod is symbolized as $\boldsymbol{F}_i \equiv \boldsymbol{F}_{(i+1)i}$ By Newton's third law of motion about action and reaction, the joint force that i-rod exerts on (i+1)-rod is $\mathbf{F}_{i(i+1)} = -\mathbf{F}_{i+1)i}(= -\mathbf{F}_i$ (**Fig. 1F**). Joint force ($\mathbf{F}_i$) can be calculated from the previously introduced given values (s_i, $\mathbf{F}_{ck,i}$, $\mathbf{F}_{b,i}$, $\tau_{c\kappa,i}$, $\tau_{b,i}$) (Details in "Joint force calculation method" of Supplementary Information). When $\mathbf{F}_0 = \mathbf{F}_n = 0$, then the total joint force that i-rod receives is $\mathbf{F}_{\text{joint},i} = \mathbf{F}_i - \mathbf{F}_{i-1}$ and the total torque caused by joint force is $\boldsymbol{\tau}_{\text{joint},i} = [\mathbf{r}_i \times (\mathbf{F}_i + \mathbf{F}_{i+1})]$ where "×" between two vectors means cross product.

As all forces and torques are found, $\mathbf{d}_c^{(t)}, \mathbf{v}_c^{(t)}, s_i^{(t)}, \omega_i^{(t)}$ can be calculated by solving translational and rotational Newtonian equations of motion with numerical integration. The time-step (Δt) used in this work is 10^{-5} sec unless otherwise noted. Because the only external force exerts on the worm is the frictional force, the equation of translational motion is $\mathbf{a}_c = \frac{\sum_i \mathbf{F}_{b,i}}{M}$. If friction coefficients ($b_\perp$, $b_\parallel$) are significantly greater than $\frac{M}{\Delta t}$, numerical integration using explicit Euler method $(\mathbf{v}_c^{(t+\Delta t)} = \mathbf{v}_c^{(t)} + \mathbf{a}_c^{(t)}\Delta t = \mathbf{v}_c^{(t)} + \frac{\sum_i \mathbf{F}_{b,i}^{(t)}}{M}\Delta t)$ becomes unstable (Butcher, 2004). So, we tackled this instability of numerical integration by developing semi-implicit Euler Method $\left(\mathbf{v}_c^{(t+\Delta t)} = \mathbf{v}_c^{(t)} + \mathbf{a}_c^{(t+\Delta t)}\Delta t \simeq \mathbf{v}_c^{(t)} + \frac{1}{1+\frac{b_\perp \Delta t}{M}} \frac{\sum_i \mathbf{F}_{b,i}^{(t)}}{M}\Delta t\right)$, which makes numerical integration stable when any frictional coefficients greater than or equal to 0 is given (Details in "Proof of numerical integration for the translational motion of a worm using semi-implicit Euler method" of Supplementary Information).

The equation of rotational motion of i-rod is $I\alpha_i = \tau_{total,i} = \tau_{b,i} + \tau_{ck,i} + \tau_{joint,i}$. When the friction-related value ($b_\parallel r^2$), elasticity-related value ($\kappa\Delta t$), or damping coefficient(c) is significantly larger than $\frac{I}{\Delta t}$, numerical integration using explicit Euler method $(\omega_i^{(t+\Delta t)} = \omega_i^{(t)} + \alpha_i^{(t)}\Delta t = \omega_i^{(t)} + \frac{\tau_{\text{total},i}^{(t)}}{I}\Delta t)$ becomes unstable (Butcher, 2004). To solve this instability, we constructed a semi-implicit Euler method for rotational motion and an error-corrected equation for angular momentum (Details in "Numerical integration of the rotational motion of i-rod using semi-implicit Euler method" and "Correction formula for the rotational inertia of the entire worm" of Supplementary Information). By using these semi-implicit Euler methods, solutions for $\mathbf{d}_c^{(t)}, \mathbf{v}_c^{(t)}, s_i^{(t)}, \omega_i^{(t)}$ of a worm at a given time can be available for the ground surface of agar whose $b_\perp$, $b_\parallel$ are significantly larger than $\frac{M}{\Delta t}$, water which has smaller friction coefficients than agar, or frictionless ground surface.

Can *C. elegans* in ElegansBot crawl or swim?

A kymogram is a heatmap that shows body angle, $\theta_i^{(t)}$ $(i \in \{1, \cdots, n-1\})$ at a given time, t. By fitting a sine function to the kymogram of previous work (Vidal-Gadea et al., 2011), we obtained linear-wavenumber(after this referred to as wavenumber) and period of *C. elegans* crawling on the agar plate and swimming in water. The wavenumber (ν) and the period (T) are, respectively, 1.832 and 1.6 (sec) on the agar plate and 0.667 and 0.4 (sec) in water. For both crawling and swimming, amplitude (A) was set to 0.6 (rad) arbitrarily to match the trajectory shown in the experimental video (Vidal-Gadea et al., 2011). Each kymogram of crawling (**Fig. 2A**) and swimming (**Fig. 2C**) was calculated by substituting amplitude (A), wavenumber (ν), and period (T) into $\theta_{\text{ctrl},i}^{(t)} = A\cos\left(2\pi(\nu(i-1)/(n-2) - t/T)\right)$.

Crawling trajectory, which performs sinusoidal locomotion in the positive x-axis direction, was obtained by inputting a crawling kymogram as $\theta_{\text{ctrl},i}^{(t)}$ input to ElegansBot (**Fig. 2B**). Regarding crawling, the head track and the tail track have similar shapes. However, the tail track is more toward the negative x-axis direction than the head track. The difference between the head and tail tracks indicates that the worm pushes the ground surface by the distance between the head track

and tail track to obtain thrust (**Fig. 2B**). Indeed, we found that the body part placed diagonally with respect to the direction of the worm's locomotion is pushing along the ground surface (Fig. S3A). The thrust force of the worm cancels out most of the drag force, which enables the worm to move at nearly constant velocity. The average velocity of the worm is 0.208 (mm/sec), which is consistent with the known values (Cohen et al., 2012; Jung et al., 2016; Omura et al., 2012; Shen et al., 2012).

In the previous work, the worm showed swimming behavior in a water droplet on an agar plate (Vidal-Gadea et al., 2011). As the friction coefficient of water is smaller than that of agar, even though the area that the worm swept was wider during swimming than crawling, the worm did not move forward much in comparison to the area it swept (**Fig. 2D**). The worm gained significant momentum in the forward direction of locomotion when the body bent in the c-shape (Fig. S3B). In contrast to crawling, during swimming, the worm did not receive constant thrust force over time. Thus, the speed of the worm exhibited significant oscillations over time (Fig. S3B), and the average velocity was 0.223 (mm/sec).

ElegansBot exhibits more complex behavior including the turn motion

Unlike previous *C. elegans* body kinematic simulation studies, our simulation can replicate the worm's behavior using a kymogram (**Fig. 3A, 3B**) derived from experimental videos. We utilized open-source software, Tierpsy Tracker (Javer et al., 2018) and WormPose (Hebert et al., 2021), to obtain the kymogram input $(\theta_{\mathrm{ctrl},i}^{(t)})$ for the ElegansBot. Through simulation, we aimed to reproduce the omega-turn and delta-turn behaviors observed in the experimental videos (Broekmans et al., 2016). When we used the vertical and horizontal friction coefficients $b_{\perp}$ and $b_{\parallel}$ on agar, as proposed in the previous work (Boyle et al., 2012), the trajectory was not accurately replicated. Given that the friction coefficients could vary depending on the concentration of the agar gel, we used $b_{\perp}/100$ and $b_{\parallel}/100$ for the vertical and horizontal friction coefficients, respectively, which resulted in a better trajectory replication (Details in "Proper Selection of Friction Coefficients" in Supplementary Information, Fig. S4~7).

The trajectory (**Fig. 3C, 3D**, Video S1, S2) obtained from ElegansBot accurately reproduces the experimental video (Broekmans et al., 2016). The changes in the direction of movement caused by turns are well replicated. Additionally, during the omega-turn or delta-turn, the body briefly performs a deep bend, and we newly discovered the mechanism that gains significant propulsion from the deep bend region to change direction using ElegansBot (**Fig. 3C, 3D**). Moreover, the ElegansBot accurately reproduces not only the turns but also complex behaviors like the sequence of forward-backward-turn-forward, also known as escaping behavior.

Additionally, we calculated the mechanical power of the worm as a quantitative indicator to explain its locomotion during sequenced locomotive behavior, based on behavior classification (forward, backward locomotion, or turn, as defined in Methods). During escaping behavior, the worm produced an average power of 2,094 fW in the initial forward locomotion, followed by an average of 16,437 fW (7.85 times that of the initial forward locomotion) in backward locomotion, and an average of 11,118 fW (5.31 times that of the initial forward locomotion) during turning (**Fig. 4A**). After turning and resuming forward locomotion, it produced an average power of 5,480 fW (2.62 times that of the initial forward locomotion). This indicates that the worm produced more power than that of initial forward locomotion to escape sudden threats. Let's denote the average of a quantity for all given i as $\langle * \rangle_i$. At the moment the worm formed a deep bend (t=11.2 sec), the average magnitude of frictional force of the body part forming the deep bend $\left(= \left\langle \left| F_{b,i}^{(t)} \right| \right\rangle_i \right.$ where i=4~15) was 3,536 pN, compared to the average magnitude of the remaining parts $\left(\left\langle \left| F_{b,i}^{(t)} \right| \right\rangle_i = 1{,}737 \text{ pN} \right.$ where i=1~3 or i=16~25), which was 2.04 times greater (**Fig. 3C**, **Fig. 4A**).

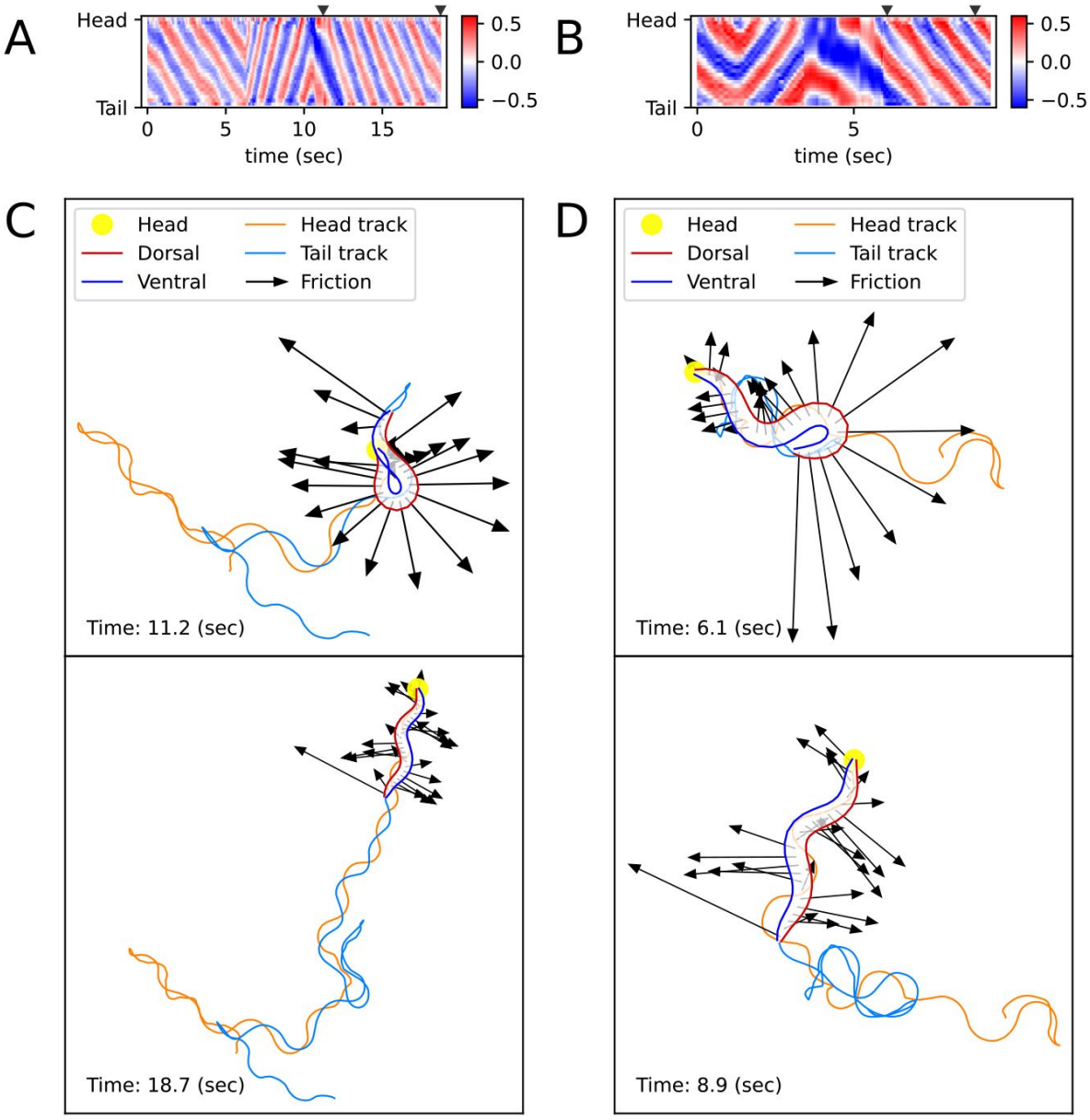

Figure 3.

Simulated locomotion from a kymogram of a real worm locomotion video.

The length and direction of a black arrow indicate the magnitude and direction of the frictional force $\left(-\mathrm{F}_{b,i}^{(t)}\right)$ that the corresponding body part, which is the starting point of the arrow, exerts on the surface. (A) escaping behavior kymogram. Triangles over the heatmap indicate the corresponding time of snapshots shown in Figure (C). (B) Delta-turn kymogram. Triangles over the heatmap indicate the corresponding time of snapshots shown in Figure (D). (C) Escaping behavior trajectory. (D) Delta-turn trajectory. The arrow length scale is different from Figure (C) to clearly show the arrows' directions and head and tail tracks. (Those videos are in Supplementary Information)

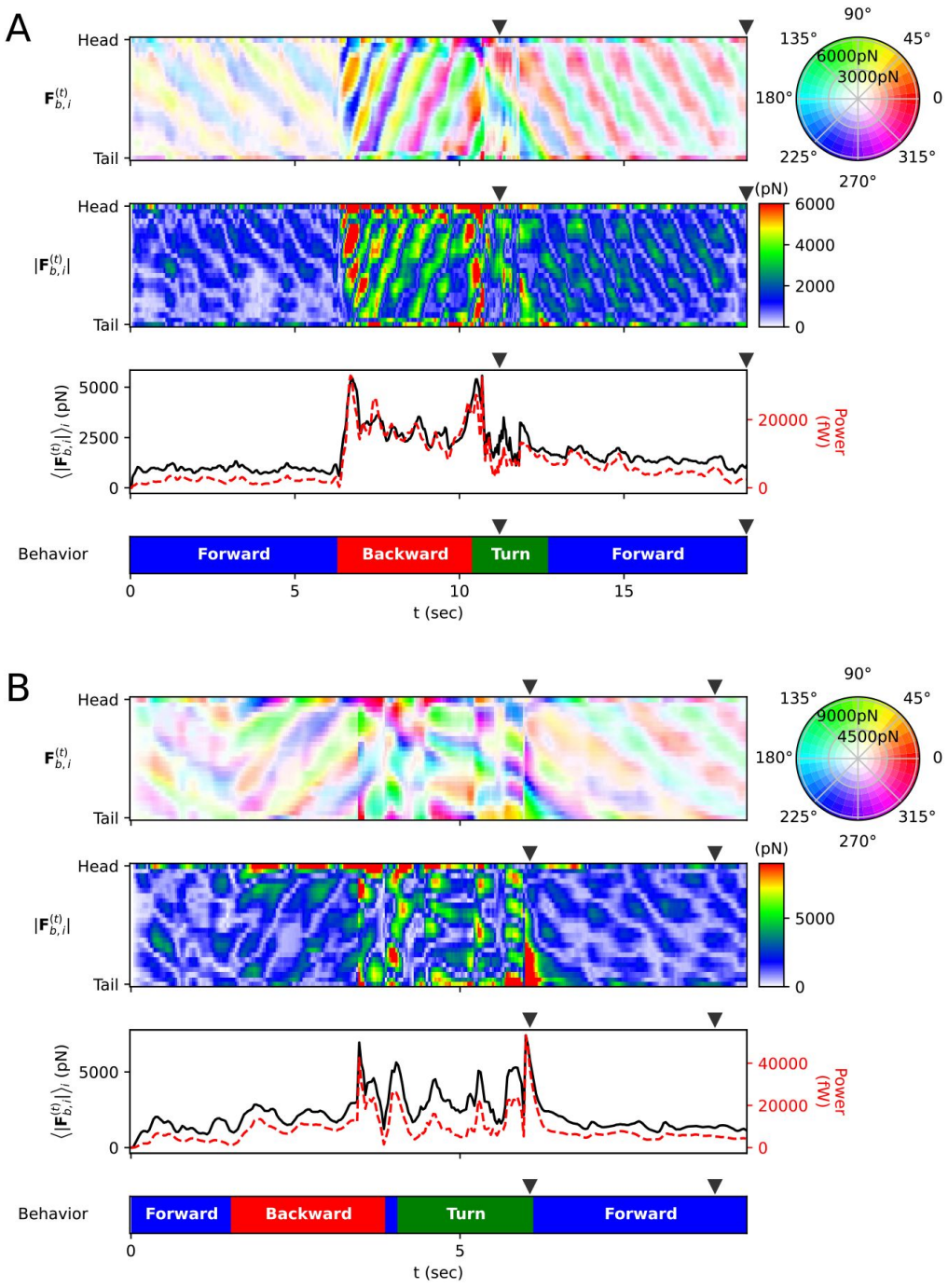

Figure 4.

Frictional force on each rod (A) Escaping behavior. The top panel represents the frictional force $\mathbf{F}_{b,i}^{(t)}$ experienced by i-rod. As indicated on the color wheel to the right, the hue of this heatmap represents the direction of the force, and the saturation represents the magnitude of the force. The second panel from the top shows the magnitude of the frictional force $\left|\mathbf{F}_{b,i}^{(t)}\right|$. The third panel from the top represents the average $\left\langle\left|\mathbf{F}_{b,i}^{(t)}\right|\right\rangle_i$ (black solid line) of each column in the middle panel and the power (red dotted line), which is the amount of energy the worm consumes per unit time. The bottom panel represents the classification of the worm's behavior (blue: forward locomotion, red: backward locomotion, green: turn) (The definitions of behavioral categories are in Methods). The triangles over each panel indicate the corresponding time of the snapshots depicted in **Fig. 3C**. (B) Delta-turn. The triangles over each panel indicate the corresponding time of the snapshots depicted in **Fig. 3D**.

We analyzed delta-turn in the same manner. The worm produced an average power of 3,514 fW in the initial forward locomotion, followed by an average of 11,176 fW (3.18 times that of the initial forward locomotion) in subsequent backward locomotion. In the relatively short duration of forward locomotion following the backward locomotion, the worm produced average power of 17,544 fW (4.99 times that of the initial forward locomotion), and an average of 13,046 fW (3.71 times that of the initial forward locomotion) during turns (**Fig. 4B**). After the turn, when resuming forward locomotion, the worm produced an average power of 6,429 fW (1.83 times that of the initial forward locomotion). At the moment the worm formed a deep bend (t=6.1 sec), the average magnitude of frictional force of the body part $(\langle|F_{b,i}^{(t)}|\rangle_i$ where i=16~25) was 10,497 pN, compared to the average magnitude of the remaining parts $(\langle|F_{b,i}^{(t)}|\rangle_i = 2{,}677$ pN where i=1~15), which was 3.92 times greater (**Fig. 3D**, **Fig. 4B**). In both escaping behavior and delta-turn, the worm consistently produced more power in the subsequent backward locomotion and turn than in the initial forward locomotion.

ElegansBot presents body shape ensembles of *C. elegans* from a shape in water en route to agar

While there have been studies on how locomotion patterns change in agar and water by merging neural and kinematic simulations (Boyle et al., 2012), there have been none that solely used kinetic simulation to analyze how speed manifests depending on the frequency and period of locomotion. We demonstrate this aspect. We studied the locomotion speed of the worm under different friction coefficients, which represent the influence of water, agar, and intermediate frictional environment, using ElegansBot. The vertical and horizontal friction coefficients in water are $b_{\text{water},\perp} = 5.2 \times 10^3$ (μg/sec) and $b_{\text{water},\parallel} = b_{\text{water},\perp}/1.5$, respectively, while in agar, these values are $b_{\text{agar},\perp} = 1.28 \times 10^8$ (μg/sec) and $b_{\text{agar},\parallel} = b_{\text{agar},\perp}/40$ (Boyle et al., 2012). For environmental index σ ∈ [0,1], we have defined the vertical and horizontal friction coefficients in the environment between water (σ = 0) and agar (σ = 1) as $b_{\sigma,\perp} = b_{\text{water},\perp}^{1-\sigma} b_{\text{agar},\perp}^{\sigma}$ and $b_{\sigma,\parallel} = b_{\text{water},\parallel}^{1-\sigma} b_{\text{agar},\parallel}^{\sigma}$, respectively.

Under an environmental index σ, for various pairs of frequency-period (ν, T) when the control angle is $\theta_{\text{ctrl},i}^{(t)} = A\cos\left(2\pi\left(\nu\frac{i-1}{23} - \frac{t}{T}\right)\right)$ (with A = 0.6 (rad)), we have found the (ν, T) that maximizes the worm's average velocity(optimal (ν, T)) (**Fig. 5A**). The optimal (ν, T) exhibits nearly linear distribution (**Fig. 5B**). We noticed a transition from swimming body shape to crawling body shape as σ varies (**Fig. 5**, S8). The optimal (ν, T) for σ=0(water) is (0.65, 0.4 sec), matching the actual (ν, T) value of swimming behavior (Vidal-Gadea et al., 2011). The optimal (ν, T) for σ=1(agar) is (1.9, 0.8 sec), and the optimal ν (1.9) matches the actual ν value (1.832) for crawling behavior (Vidal-Gadea et al., 2011), with the optimal T (0.8 sec) being half the actual T value (1.6 sec).

We wanted to understand the impact of the environmental index σ not only on forward locomotion but also on sequenced locomotive behavior. First, we analyzed the effect of the environmental index σ on escaping behavior as follows. Let's denote the set of a quantity for all pair of index i and time t as $\{*\}_{i,t}$. When the escaping behavior kymogram input $\{\theta_{\text{ctrl},i}^{(t)}\}_{i,t}$ was same as **Fig. 3A**, we explored the effect of vertical and horizontal friction coefficients on the worm's motion. Where σ ranged from 1.0 to 0, the trajectory varied with σ (Fig. S9A), and $E_\theta = \langle|\theta_i^{(t)} - \theta_{\text{ctrl},i}^{(t)}|\rangle_{i,t}$ decreased as σ decreased (Fig. S9B). From σ = 1.0 to 0.1, the total absolute angular change $(\mathcal{S} = \sum_{t=0}^{T-\Delta t}\left|\langle s_i^{(t+\Delta t)}\rangle_i - \langle s_i^{(t)}\rangle_i\right|$ where T is total time of the experimental video.) increased as σ decreased. However, from σ = 0.7 to 0, $\mathcal{S}$ remained constant within the error of 0.33 rad, and the total traveled distance $(\sum_t|\mathbf{v}_c^{(t)}\Delta t|)$ decreased as σ decreased. The maximum total traveled distance was at σ =0.8. Using the same analysis method with the kymogram input $\{\theta_{\text{ctrl},i}^{(t)}\}_{i,t}$ same as **Fig. 3B**, we analyzed the impact of the environmental index σ on delta-turn. Where σ

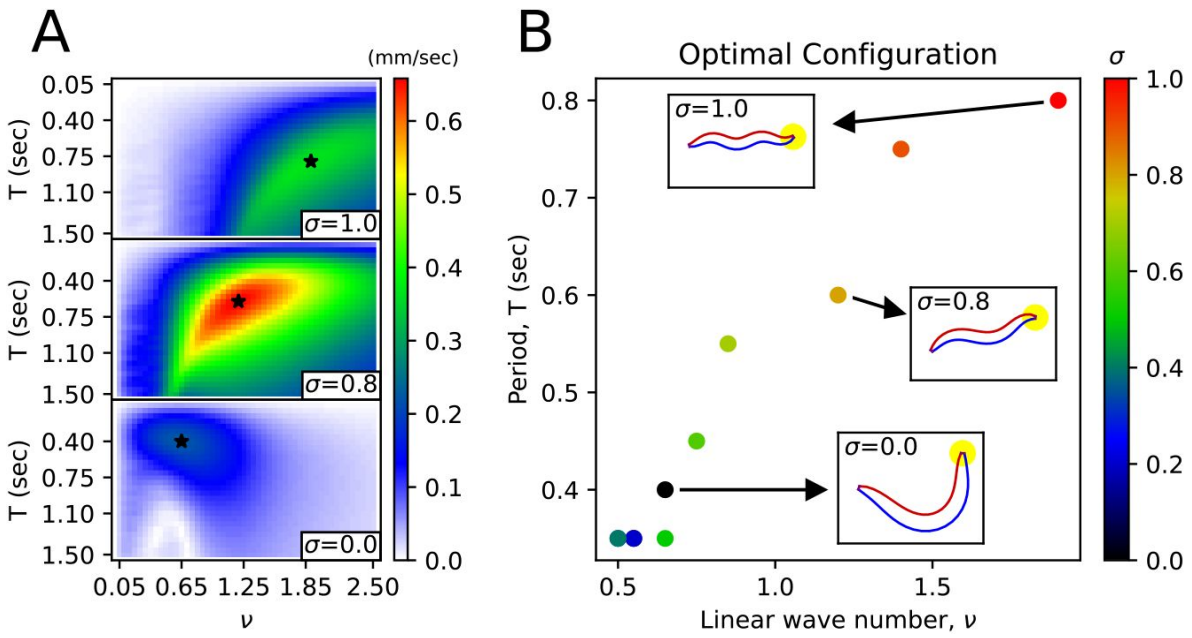

Figure 5.

Body shape transition from the shape in water to the shape in agar.

Average velocity of the worm as a function of wavenumber (*ν*) and period (*T*) for a given friction coefficient. The star symbol indicates the pair of (*ν, T*) that maximizes the worm's average velocity. (B) For each environmental index σ, the pair of (*ν, T*) that maximizes the worm's average velocity. The worm figures inside the small rectangles pointed to by the arrows represent the body shape corresponding to the respective (*ν, T*) pair.

, we explored the effect of vertical and horizontal friction coefficients on the worm's motion. Where σ ranged from 1.0 to 0, the trajectory varied with σ (Fig. S9A), and $E_\theta = \langle |\theta_i^{(t)} - \theta_{\mathrm{ctrl},i}^{(t)}| \rangle_{i,t}$ decreased as σ decreased (Fig. S9B). From σ = 1.0 to 0.1, the total absolute angular change ($\mathcal{S} = \sum_{t=0}^{T-\Delta t} \left| \langle s_i^{(t+\Delta t)} \rangle_i - \langle s_i^{(t)} \rangle_i \right|$ where T is total time of the experimental video.) increased as σ decreased. However, from σ = 0.7 to 0, $\mathcal{S}$ remained constant within the error of 0.33 rad, and the total traveled distance ($\sum_t |\mathbf{v}_c^{(t)} \Delta t|$) decreased as σ decreased. The maximum total traveled distance was at σ =0.8. Using the same analysis method with the kymogram input $\{\theta_{\mathrm{ctrl},i}^{(t)}\}_{i,t}$ same as **Fig. 3B**, we analyzed the impact of the environmental index σ on delta-turn. Where σ ranged from 1.0 to 0, the trajectory varied with σ (Fig. S10A), and E_θ also decreased as σ decreased (Fig. S10B). From σ = 1 to 0.6, $\mathcal{S}$ increased as σ decreased. From σ = 0.6 to 0, $\mathcal{S}$ decreased as σ decreased. The maximum total traveled distance was at σ = 0.9.From σ = 0.9 to 0, the total traveled distance decreased as σ decreased.

Discussion

ElegansBot is an advanced kinetic simulator that reproduces *C. elegans*' various locomotion

The known crawling speed range of *C. elegans* (Cohen et al., 2012; Jung et al., 2016; Omura et al., 2012; Shen et al., 2012) matches the speed in our simulation. The force dispersion pattern of the forward movement of a snake (Hu et al., 2009) is similar to the force dispersion pattern of crawling in our model, where the body part placed diagonally to the direction of movement generates thrust. The head and tail tracks of our simulation resemble the trace left on the agar plate by *C. elegans* during locomotion (Yeon et al., 2018), providing evidence of the mechanism where *C. elegans* moves forward by pushing along the ground surface. Given that friction and elasticity coefficients can vary between experiments, the appropriate selection of these values allows the trajectories of omega-turns and delta-turns in our simulations to match the experimental videos (Broekmans et al., 2016). Previous work (Boyle, 2009; Boyle et al., 2012) eliminated inertia from the equations of motion, but our simulation includes it, allowing calculation even in cases where inertia is significant due to low friction coefficients. Using the crawling and swimming wavenumbers and periods from the experiments (Vidal-Gadea et al., 2011), we computed sine functions to create trajectories for crawling and swimming. We also analyzed how friction forces act on the worm during crawling and swimming, studying how the worm gains propulsion. We demonstrated that we could reproduce various locomotion observed in experimental videos, such as forward-backward-(omega turn)-forward constituting escaping behavior and delta-turn navigation, by providing the kymogram obtained from representative physical values from the experimental videos, as well as the kymogram obtained from a program (Hebert et al., 2021; Javer et al., 2018) extracting the body angles from actual experimental videos into ElegansBot. Our established Newtonian equations of motion are accurate and robust, suggesting that not only does our simulation replicate the experimental videos, but it also provides credible estimates for detailed forces.

ElegansBot will serve as a strong bridge for enhancing the knowledge in "from-synapse-to-behavior" research

Our method could be used for kinetic analysis of behaviors not covered in this paper. It could also be used when analyzing behavior changes caused by mutation or ablation experiments. Given that our simulation allows for kinetic analysis, it could be used to calculate the energy expended by the worm during locomotion, serving as an activity index. Our simulation only requires the body angles as input data, so even if the video angle shifts and trajectory information is lost, the trajectory can be recovered from the kymogram. Our simulation could also be used when studying

neural circuit models of *C. elegans*. It could be used to check how signals from neural network models manifest as behaviors which is a needed function from previous work (Sakamoto et al., 2021), and it could be used when studying compound models of neural circuits and bodies. For example, when creating models that receive proprioception input based on body shape (Boyle et al., 2012; Ekeberg, 1993; Izquierdo & Beer, 2018; Niebur & Erdös, 1991), our method could be used. Finally, our method could be used in general for the broad utility to analyze the motion of rod-shaped animals like snakes or eels and to simulate the motion of rod-shaped robots.

Methods

1. Frequency and wavelength of *C. elegans* locomotion

Sine function fitting was applied to the crawling and swimming kymograms (Vidal-Gadea et al., 2011) to determine the frequency and wavelength of *C. elegans* locomotion on agar and water.

2. *C. elegans* locomotion videos

Videos of *C. elegans*' escaping behavior and foraging behavior were obtained from previous work (Broekmans et al., 2016). A single representative video out of a total of one hundred escaping behavior videos was used as data in this paper. Additionally, only the delta-turning portion of the foraging behavior videos was cut out and used as data in this paper.

3. Obtaining kymograms from video

The following method was used to extract the kymogram from the video of *C. elegans*: The body angles and midline were extracted using Tierpsy Tracker (Javer et al., 2018) from the original video where the worm is locomoting. Tierpsy Tracker failed to extract the midline of the worm when the body parts meet or the worm is coiled. The midline information of the frames successfully predicted by Tierpsy Tracker and the original video information were used as ground truth training data for a program called WormPose (Hebert et al., 2021). WormPose trained an artificial neural network to extract the body angles and midline of a coiled worm using a generative method based on the input data. The body angles were extracted from the original video using the trained WormPose program. For the frames where Tierpsy Tracker failed to extract the body angles, it was replaced with the body angles extracted by WormPose. Nonetheless, there were frames where the body angle extraction failed. If the period of failed body angle prediction was continuously less than three frames (about 0.01 seconds), the body angles for that period was predicted using linear interpolation.

4. Program code and programming libraries

Equations for the chain model, friction model, muscle model, and numerical integration that constitute the ElegansBot were designed from the body angle information and kymogram that change every moment of time. Python (van Rossum, 1995) version 3.8 was used to implement the equations constituting ElegansBot as a program. NumPy (Harris et al., 2020) version 1.19 was used for numerical calculations, and Numba (Lam et al., 2015) version 0.54 was used for CPU calculation acceleration. SciPy (Virtanen et al., 2020) version 1.5 was used for curve fitting and Savitzky-Golay filter (Savitzky & Golay, 1964) to classify the worm's behavioral categories. The Matplotlib (Hunter, 2007) library was used to represent *C. elegans*' body pose and trajectory in figures and videos. The program code used in the research can be obtained from the open database GitHub (*https://github.com/taegonchung/elegansbot*) or Python software repository PyPI (*https://pypi.org/project/ElegansBot/*), and the web live demo can be found at GitHub Page (*https://taegonchung.github.io/elegansbot/*). This code calculated the ElegansBot simulation of 10 seconds of simulation time in about 10 seconds of run-time on an Intel E3-1230v5 CPU.

5. Physical constants of the ground surface

The friction coefficient values for the ground surface where *C. elegans* crawled and swam and the elastic and damping coefficients of *C. elegans* muscles were obtained from previous work (Boyle et al., 2012). The muscle elasticity and damping coefficients were converted into coefficients for the damped torsional spring to be used in our model (Details in "Worm's mass, actuator elasticity coefficient, and damping coefficient" of Supplementary Information).

6. Defining Behavioral Categories

We determined the classification of the worm's behavior over time as follows. Let $\xi_i \equiv (i-1)/(n-2)$ (i.e., $0 \le \xi_i \le 1$). We defined a sine function fitting for the body angle $\theta_i^{(t)}$ as $\hat{\theta}_i^{(t)} = A^{(t)}\sin\left(\left(2\pi/\lambda^{(t)}\right)\left(\xi_i - \xi_0^{(t)}\right)\right) + \theta_0^{(t)}$ (where $A^{(t)} \ge 0$ and $0 \le \xi_0^{(t)} < \lambda^{(t)}$). Let us denote the set of a quantity for all i as $\{*\}_i$. For a given time t, by curve fitting the function $\hat{\theta}_i^{(t)}$ to the set of body angles $\{\theta_i^{(t)}\}_i$, we can obtain the parameters $\left(A^{(t)}, \lambda^{(t)}, \xi_0^{(t)}, \theta_0^{(t)}\right)$ (Fig. S11). For curve fitting, we used 'curve_fit' from the scipy library (Virtanen et al., 2020). 'curve_fit' requires the function to be fitted, the data, and the initial guess values of the function parameters. Therefore, we determined the initial guess values $\left(\hat{A}^{(t)}, \hat{\lambda}^{(t)}, \hat{\xi}_0^{(t)}, \hat{\theta}_0^{(t)}\right)$ as follows. For $t = 0$, we calculated $\left(\hat{A}^{(0)}, \hat{\lambda}^{(0)}, \hat{\xi}_0^{(0)}, \hat{\theta}_0^{(0)}\right)$ using the following equations:

$$\begin{aligned}
\hat{A}^{(0)} &= \frac{1}{2}\left(\max_i\left(\theta_i^{(0)}\right) - \min_i\left(\theta_i^{(0)}\right)\right) \\
\hat{\lambda}^{(0)} &= \frac{2}{n-2}\left(\operatorname{argmax}_i\left(\theta_i^{(0)}\right) - \operatorname{argmin}_i\left(\theta_i^{(0)}\right)\right) \\
\hat{\xi}_0^{(0)} &= \frac{1}{n-2}\left(\operatorname{argmax}_i\left(\theta_i^{(0)}\right)\right) - \frac{\hat{\lambda}^{(0)}}{4} \\
\hat{\theta}_0^{(0)} &= \frac{1}{n-1}\left(\sum_i \theta_i^{(0)}\right)
\end{aligned}$$

Using these initial guess values, we curve fitted $\hat{\theta}_i^{(0)}$ to $\{\theta_i^{(0)}\}_i$ to obtain $\left(A^{(0)}, \lambda^{(0)}, \xi_0^{(0)}, \theta_0^{(0)}\right)$. For $t \ge \Delta t$, we obtained the initial guess values for curve fitting as $\hat{A}^{(t)} = A^{(t-\Delta t)}$, $\hat{\lambda}^{(t)} = \lambda^{(t-\Delta t)}$, $\hat{\xi}_0^{(t)} = \xi_0^{(t-\Delta t)}$, $\hat{\theta}_0^{(t)} = \xi_0^{(t-\Delta t)}$. Then, using these initial guess values, we curve fitted $\hat{\theta}_i^{(t)}$ to $\{\theta_i^{(t)}\}_i$ to obtain $\left(A^{(t)}, \lambda^{(t)}, \xi_0^{(t)}, \theta_0^{(t)}\right)$. Since the phase $\xi_0^{(t)}$ is not continuous for all time t, we defined a continuous value $\tilde{\xi}_0^{(t)}$ for all time t as follows (Fig. S11):

$$\tilde{\xi}_0^{(t)} = \begin{cases} \xi_0^{(t)} & \text{if } t = 0 \\ \xi_0^{(t)} - \xi_0^{(t-\Delta t)} + \tilde{\xi}_0^{(t-\Delta t)} & \text{if } t > 0 \text{ and } -\dfrac{\lambda^{(t)}}{2} \le \xi_0^{(t)} - \xi_0^{(t-\Delta t)} \le \dfrac{\lambda^{(t)}}{2} \\ \xi_0^{(t)} - \xi_0^{(t-\Delta t)} + \tilde{\xi}_0^{(t-\Delta t)} + \lambda^{(t)} & \text{if } t > 0 \text{ and } \xi_0^{(t)} - \xi_0^{(t-\Delta t)} < -\dfrac{\lambda^{(t)}}{2} \\ \xi_0^{(t)} - \xi_0^{(t-\Delta t)} + \tilde{\xi}_0^{(t-\Delta t)} - \lambda^{(t)} & \text{if } t > 0 \text{ and } \dfrac{\lambda^{(t)}}{2} < \xi_0^{(t)} - \xi_0^{(t-\Delta t)} \end{cases}$$

To obtain the derivatives of the noise-reduced smoothed values $\bar{\xi}_0^{(t)}$ and $\bar{\theta}_0^{(t)}$ for the raw data $\tilde{\xi}_0^{(t)}$ and $\theta_0^{(t)}$, respectively, we applied a Savitzky-Golay filter (Savitzky & Golay, 1964; Virtanen et al., 2020). This filter, set with a smoothing time window of 0.5 second, a polynomial order of 2, and a derivative order of 1, yielded $\frac{d\bar{\xi}_0^{(t)}}{dt}$ and $\frac{d\bar{\theta}_0^{(t)}}{dt}$. We then calculated the temporal integrals $\xi'^{(\zeta)}_0 \equiv \sum_{t=0}^{\zeta} \frac{d\bar{\xi}_0^{(t)}}{dt}$ and $\theta'^{(\zeta)}_0 \equiv \sum_{t=0}^{\zeta} \frac{d\bar{\theta}_0^{(t)}}{dt}\Delta t$. Let us denote the average of a quantity for all time t as $\langle * \rangle_t$. We

calculated $\bar{\xi}_0^{(t)} = \xi'^{(t)}_0 - \langle \xi'^{(t)}_0 \rangle_t + \langle \tilde{\xi}_0^{(t)} \rangle_t$ and $\bar{\theta}_0^{(t)} = \theta'^{(t)}_0 - \langle \theta'^{(t)}_0 \rangle_t + \langle \theta_0^{(t)} \rangle_t$ (Fig. S11). Finally, we defined the worm's behavior classification as turn when $\bar{\theta}_0^{(t)} < -0.07$ as forward locomotion when $\bar{\theta}_0^{(t)} \geq -0.07$ and $\frac{d\bar{\xi}_0^{(t)}}{dt} > 0$, and as backward locomotion when $\bar{\theta}_0^{(t)} \geq -0.07$ and $\frac{d\bar{\xi}_0^{(t)}}{dt} \leq 0$ (Fig. S11).

Acknowledgements

This work is supported by the p-CoE program of DGIST 23-CoE-BT-01. We also acknowledge Prof. Kyuhyung Kim for fruitful discussions on experiments of C. elegans.

References

Boyle J. H. (2009) **C. elegans locomotion: An integrated approach**

Boyle J. H., Berri S., Cohen N. (2012) **Gait Modulation in C. elegans: An Integrated Neuromechanical Model** *Frontiers in Computational Neuroscience* **6** https://doi.org/10.3389/fncom.2012.00010

Broekmans O. D., Rodgers J. B., Ryu W. S., Stephens G. J. (2016) **Resolving coiled shapes reveals new reorientation behaviors in C. elegans** *eLife* **5** https://doi.org/10.7554/eLife.17227

Butcher J. C. (2004) **Numerical Methods for Ordinary Differential Equations**

Cohen E., Yemini E., Schafer W., Feitelson D. G., Treinin M. (2012) **Locomotion analysis identifies roles of mechanosensory neurons in governing locomotion dynamics of C. elegans** *Journal of Experimental Biology* **215**:3639–3648 https://doi.org/10.1242/jeb.075416

Cook S. J. *et al.* (2019) **Whole-animal connectomes of both Caenorhabditis elegans sexes** *Nature* **571**:63–71 https://doi.org/10.1038/s41586-019-1352-7

Ekeberg O. (1993) **A combined neuronal and mechanical model of fish swimming** *Biological Cybernetics* **12**

Hall D. H., Altun Z. F. (2008) **C. elegans Atlas**

Harris C. R. *et al.* (2020) **Array programming with NumPy** *Nature* **585** https://doi.org/10.1038/s41586-020-2649-2

Hebert L., Ahamed T., Costa A. C., O'Shaughnessy L., Stephens G. J. (2021) **WormPose: Image synthesis and convolutional networks for pose estimation in C. elegans** *PLOS Computational Biology* **17** https://doi.org/10.1371/journal.pcbi.1008914

Hill A. V. (1937) **The heat of shortening and the dynamic constants of muscle** *Proceedings of the Royal Society of London. Series B - Biological Sciences* **126**:136–195 https://doi.org/10.1098/rspb.1938.0050

Hu D. L., Nirody J., Scott T., Shelley M. J. (2009) **The mechanics of slithering locomotion** *Proceedings of the National Academy of Sciences* **106**:10081–10085 https://doi.org/10.1073/pnas.0812533106

Hunter J. D. (2007) **Matplotlib: A 2D Graphics Environment** *Computing in Science & Engineering* **9**:90–95 https://doi.org/10.1109/MCSE.2007.55

Izquierdo E. J., Beer R. D. (2018) **From head to tail: A neuromechanical model of forward locomotion in Caenorhabditis elegans** *Philosophical Transactions of the Royal Society B: Biological Sciences* **373** https://doi.org/10.1098/rstb.2017.0374

Javer A. *et al.* (2018) **An open-source platform for analyzing and sharing wormbehavior data** *Nature Methods* **15** https://doi.org/10.1038/s41592-018-0112-1

Jung J., Nakajima M., Takeuchi M., Najdovski Z., Huang Q., Fukuda T. (2016) **Microfluidic Device to Measure the Speed of C. elegans Using the Resistance Change of the Flexible Electrode** *Micromachines* **7** https://doi.org/10.3390/mi7030050

Lam S. K., Pitrou A., Seibert S. (2015) **Numba: A LLVM-based Python JIT compiler** *Proceedings of the Second Workshop on the LLVM Compiler Infrastructure in HPC* :1–6 https://doi.org/10.1145/2833157.2833162

Niebur E., Erdös P. (1991) **Theory of the locomotion of nematodes: Dynamics of undulatory progression on a surface** *Biophysical Journal* **60**:1132–1146 https://doi.org/10.1016/S0006-3495(91)82149-X

Omura D. T., Clark D. A., Samuel A. D. T., Horvitz H. R. (2012) **Dopamine Signaling Is Essential for Precise Rates of Locomotion by C. elegans** *PLOS ONE* **7** https://doi.org/10.1371/journal.pone.0038649

Sakamoto K., Soh Z., Suzuki M., Iino Y., Tsuji T. (2021) **Forward and backward locomotion patterns in C. elegans generated by a connectome-based model simulation** *Scientific Reports* **11** https://doi.org/10.1038/s41598-021-92690-2

Savitzky Abraham., Golay M. J. E. (1964) **Smoothing and Differentiation of Data by Simplified Least Squares Procedures** *Analytical Chemistry* **36**:1627–1639 https://doi.org/10.1021/ac60214a047

Shen X. N., Sznitman J., Krajacic P., Lamitina T., Arratia P. E. (2012) **Undulatory Locomotion of Caenorhabditis elegans on Wet Surfaces** *Biophysical Journal* **102**:2772–2781 https://doi.org/10.1016/j.bpj.2012.05.012

van Rossum G. (1995) **Python reference manual (Issue R 9525). CWI**

Vidal-Gadea A. *et al.* (2011) **Caenorhabditis elegans selects distinct crawling and swimming gaits via dopamine and serotonin** *Proceedings of the National Academy of Sciences* **108**:17504–17509 https://doi.org/10.1073/pnas.1108673108

Virtanen P. *et al.* (2020) **SciPy 1.0: Fundamental algorithms for scientific computing in Python** *Nature Methods* **17** https://doi.org/10.1038/s41592-019-0686-2

White J. G., Southgate E., Thomson J. N., Brenner S. (1986) **The Structure of the Nervous System of the Nematode Caenorhabditis elegans** *Philosophical Transactions of the Royal Society of London. Series B, Biological Sciences* **314**:1–340

Yeon J., Kim J., Kim D.-Y., Kim H., Kim J., Du E. J., Kang K., Lim H.-H., Moon D., Kim K. (2018) **A sensory-motor neuron type mediates proprioceptive coordination of steering in C. elegans via two TRPC channels** *PLOS Biology* **16** https://doi.org/10.1371/journal.pbio.2004929

Article and author information

Taegon Chung

Department of Brain Sciences, Daegu Gyeongbuk Institute of Science and Technology, Korea
ORCID iD: 0009-0004-2335-3500

Iksoo Chang
Department of Brain Sciences, Daegu Gyeongbuk Institute of Science and Technology, Korea
ORCID iD: 0000-0003-0594-8784

Sangyeol Kim
Department of Brain Sciences, Daegu Gyeongbuk Institute of Science and Technology, Korea
For correspondence: sykim@dgist.ac.kr
ORCID iD: 0009-0001-3200-9726

Copyright

© 2023, Chung et al.

This article is distributed under the terms of the Creative Commons Attribution License, which permits unrestricted use and redistribution provided that the original author and source are credited.

Editors

Reviewing Editor
Gordon Berman
Emory University, Atlanta, United States of America

Senior Editor
Aleksandra Walczak
École Normale Supérieure - PSL, Paris, France

Reviewer #1 (Public Review):

Summary:

This work describes a simple mechanical model of worm locomotion, using a series of rigid segments connected by damped torsional springs and immersed in a viscous fluid. It uses this model to simulate forward crawling movement, as well as omega turns.

Strengths:

The primary strength is in applying a biomechanical model to omega-turn behaviors. The biomechanics of nematode turning behaviors are relatively less well described and understood than forward crawling, and the increase in power during omega turns is one of the more novel results. The model itself may be a useful implementation to other researchers, particularly owing to its simplicity.

Weaknesses:

The strength of the model presented in this work relative to prior approaches is not well supported, and in general the paper would be improved with a better description of the broader context of existing modeling literature related to undulatory locomotion. This paper claims to improve on previous approaches to taking body shapes as inputs. However, the sole nematode model cited aims to do something different, and arguably more significant, which is to use experimentally derived parameters to model both the neural circuits that induce locomotion as well as the biomechanics and to subsequently compare the model to experimental data. Other modeling approaches do take experimental body kinematics as inputs and use them to produce force fields, however, they are not cited or discussed. Finally, the overall novelty of the approach is questionable. A functionally similar approach was

developed in 2012 to describe worm locomotion in lattices (Majmudar, 2012, Roy. Soc. Int.), which is not discussed and would provide an interesting comparison and needed context.

In some sense, because the model takes kinematics as an input and uses previously established techniques to model mechanics, it is unsurprising that it can reproduce experimentally observed kinematics, however, the forces calculated and the variation of parameters could be of interest, but other methods derived from kinematics could provide similar results. It is unclear what the predictive power of the model is.

Relatedly, a justification of why the drag coefficients had to be changed by a factor of 100 should be explored. Plate conditions are difficult to replicate and the rheology of plates likely depends on several factors, but is for example, changes in hydration level likely to produce a 100-fold change in drag? or something more interesting/subtle within the model producing the discrepancy?

Finally, the language used to distinguish different modeling approaches was often unclear. For example, it was unclear in what sense the model presented in Boyle, 2012 was a "kinetic model" and in many situations, it appeared that the term kinematic might have been more appropriate. Other phrases like "frictional forces caused by the tension of its muscles" were unclear at first glance, and might benefit from revision and more canonical usage of terms.

https://doi.org/10.7554/eLife.92562.2.sa2

Reviewer #2 (Public Review):

Summary:

Developing a mechanical model of C. elegans is difficult to do from basic principles because it moves at low (but not very small) Reynolds number, is itself visco-elastic, and often is measured moving at a solid/liquid interface. The EleganSBot is a good first step at a kinetic model that reproduces a wide range of C. elegans motility behavior.

Strengths:

The model is general due to its simplicity and likely useful for various undulatory movements. The model reproduces experimental movement data using realistic physical parameters (e.g. drags, forces, etc). The model is predictive (semi?) as shown in the liquid to solid gait transition. The model is straightforward in implementation and so likely is adaptable to modification and addition of control circuits.

Comments on revised version:

This is a revised manuscript. I'm happy with the changes made, including the specific responses to my previous concerns.

https://doi.org/10.7554/eLife.92562.2.sa1

Reviewer #3 (Public Review):

A mechanical model of C. elegans, embedded in a resistive force environment, is used to calculate input torque patterns required to generate output curvature patterns and coordinates, corresponding to a number of different locomotion behaviors in C. elegans.

Strengths:

The use of a mechanical model to study a variety of locomotor sequences and the grounding in empirical data are strengths. The matching of speeds (though requiring adjusted drag coefficients) is a strength.

Weaknesses:

The paper lacks evidence of numerical validation or comparison with the results and tools in the literature. E.g. is it surprising that the uniform torque distribution yields maximal speed? What is the relation between input and output data? How does the input-output relation depend on the parameters of the model? What novel model predictions are made?

In particular, if validated, the breakdown of drag forces and torque distributions during forward locomotion and turning behaviors may be interesting to compare to predictions by other tools, and to empirical measurement. One caveat is that the worm touches itself during such turns, and even crosses over itself in delta turns, and so the estimated drag coefficients and the resultant mechanical forces are likely incorrect.

https://doi.org/10.7554/eLife.92562.2.sa0

Author Response

The following is the authors' response to the original reviews.

> ***Reviewer #1***
>
> ***Public Review***
>
> *Summary:*
>
> *(1) This work describes a simple mechanical model of worm locomotion, using a series of rigid segments connected by damped torsional springs and immersed in a viscous fluid.*
>
> *(2) It uses this model to simulate forward crawling movement, as well as omega turns.*
>
> *Strengths:*
>
> *(3) The primary strength is in applying a biomechanical model to omega-turn behaviors.*
>
> *(4) The biomechanics of nematode turning behaviors are relatively less well described and understood than forward crawling.*
>
> *(5) The model itself may be a useful implementation to other researchers, particularly owing to its simplicity.*
>
> *Weaknesses:*
>
> *(6) The strength of the model presented in this work relative to prior approaches is not well supported, and in general, the paper would be improved with a better description of the broader context of existing modeling literature related to undulatory locomotion.*
>
> *(7) This paper claims to improve on previous approaches to taking body shapes as inputs.*
>
> *(8) However, the sole nematode model cited aims to do something different, and arguably more significant, which is to use experimentally derived parameters to model both the neural circuits that induce locomotion as well as the biomechanics and to subsequently compare the model to experimental data.*

> *(9) Other modeling approaches do take experimental body kinematics as inputs and use them to produce force fields, however, they are not cited or discussed.*
>
> *(10) Finally, the overall novelty of the approach is questionable.*
>
> *(11) A functionally similar approach was developed in 2012 to describe worm locomotion in lattices (Majmudar, 2012, Roy. Soc. Int.), which is not discussed and would provide an interesting comparison and needed context.*

9-11: The paper you recommended and our manuscript have some similarities and differences.

Similarities

Firstly, the components constituting the worm are similar in both models. EleganSBot models the worm as a chain of n rods, while the study by Majmudar et al. (2012) models it as a chain of n beads. Each bead in the Majmudar et al. model has a directional vector, making it very similar to EleganSBot's rod. However, there's a notable difference: in the Majmudar et al. model, each bead has an area for detecting contact between the obstacle and the bead, while in EleganSBot, the rod does not feature such an area.

Secondly, the types of forces and torques acting on the components constituting the worm are similar. Each rod in EleganSBot receives frictional force, muscle force, and joint force. Each bead in the Majmudar et al. model receives a constraint force, viscous force, and a repulsive force from obstacles. Each rod in EleganSBot receives frictional torque, muscle torque, and joint torque. Each bead in the Majmudar et al. model receives elastic torque, constraint torque, drive torque, and viscous torque. The Majmudar et al. model's constraint force and torque are similar to EleganSBot's joint force and torque in that they prevent two connected components of the worm from separating. The Majmudar et al. model's viscous force and torque are similar to EleganSBot's frictional force and torque in that they are forces exchanged between the worm and its surrounding environment (ground surface). The Majmudar et al. model's drive torque is similar to EleganSBot's muscle force and muscle torque as a cause of the worm's motion. However, unlike EleganSBot, the Majmudar et al. model did not consider the force generating the drive torque, and there are differences in how each force and torque is calculated. This will be discussed in more detail below.

Differences

Firstly, the medium in which the worm locomotes is different. EleganSBot is a model describing motion in a homogeneous medium like agar or water without obstacles, while the Majmudar et al. model describes motion in water with circular obstacles fixed at each lattice point. This is because the purposes of the models are different. EleganSBot analyzes locomotion patterns based on the friction coefficient, while the Majmudar et al. model analyzes locomotion patterns based on the characteristics of the obstacle lattice, such as the distance between obstacles. Also, for this reason, the Majmudar et al. model's bead, unlike EleganSBot's rod, receives a repulsive force from obstacles.

Secondly, the specific methods of calculating similar types of forces differ. EleganSBot calculates joint forces by substituting frictional forces, muscle forces, frictional torques, and muscle torques into an equation derived from differentiating a boundary condition equation twice over time, where two neighboring rods always meet at one point. This involves determining the process through which various forces and torques are transmitted across the worm. Specifically, it entails calculating how the frictional forces and torques, as well as the muscle forces and torques acting on each rod, are distributed throughout the entire length of the worm. In contrast, The Majmudar et al. model uses Lagrange multipliers method based on a boundary condition that the curve length determined by each bead's tangential angle does

not change, to calculate the constraint force and torque before calculating the drive torque and viscous force. This implies that the Majmudar et al. model did not consider the mechanism by which the drive torque and viscous force received by one bead are distributed throughout the worm. EleganBot's rod receives an anisotropic Stokes frictional force from the ground surface, while the Majmudar et al. model considered the frictional force according to the Navier-Stokes equation for incompressible fluid, assuming the fluid velocity at the bead's location as the bead's velocity.

Thirdly, unlike the Majmudar et al. model, EleganBot considers the inertia of the worm components. Therefore, EleganBot can simulate regardless of how low or high the ground surface's friction coefficient is. the Majmudar et al. model is not like this.

> *(12) The idea of applying biomechanical models to describe omega turns in C. elegans is a good one, however, the kinematic basis of the model as used in this paper (the authors do note that the control angle could be connected to a neural model, but don't do so in this work) limits the generation of neuromechanical control hypotheses.*

8, 12: We do not agree with the claim that EleganBot could limit other researchers in generating neuromechanical control hypotheses. The term θ_("ctrl" ,i)^((t)) used in our model is designed to be replaceable with neuromechanical control in the future.

> *(13) The model may provide insights into the biomechanics of such behaviors, however, the results described are very minimal and are purely qualitative.*
>
> *(14-1) Overall, direct comparisons to the experiments are lacking or unclear.*

14-1: If you look at the text explaining Fig. 2 and 5 (Fig. 2 and 4 in old version), it directly compares the velocity, wave-number, and period as numerical indicators representing the behavior of the worm, between the experiment and EleganBot.

> *(14-2) Furthermore, the paper claims the value of the model is to produce the force fields from a given body shape, but the force fields from omega turns are only pictured qualitatively.*

13, 14-2: We gratefully accept the point that our analysis of the omega-turn is qualitative. Therefore, we have conducted additional quantitative analysis on the omega-turn and inserted the results into the new Fig. 4. We have considered the term 'Force field' as referring to the force vector received by each rod. We have created numerical indicators representing various behaviors of the worm and included them in the revised manuscript.

> *(15) No comparison is made to other behaviors (the force experienced during crawling relative to turning for example might be interesting to consider) and the dependence of the behavior on the model parameters is not explored (for example, how does the omega turn change as the drag coefficients are changed).*

Thank you for the great idea. To compare behaviors, first, a clear criterion for distinguishing behaviors is needed. Therefore, we have created a new mathematical definition for behavior classification in the revised manuscript (“Defining Behavioral Categories” in Method). After that, we compared the force and power (energy consuming rate) between each forward locomotion, backward locomotion, and omega-turn (Fig. 4). And in the revised manuscript, we newly analyzed how the turning behavior changes with variations in the friction coefficients in Figs. S4-S7.

> *(16) If the purpose of this paper is to recapitulate the swim-to-crawl transition with a simple model, and then apply the model to new behaviors, a more detailed analysis of*

> *the behavior of the model variables and their dependence on the variables would make for a stronger result.*

In our revised manuscript, we have quantitatively analyzed the changes occurring in turning behavior from water to agar, and the results are presented in Figs. S9 and S10.

> *(17) In some sense, because the model takes kinematics as an input and uses previously established techniques to model mechanics, it is unsurprising that it can reproduce experimentally observed kinematics, however, the forces calculated and the variation of parameters could be of interest.*
>
> *(18) Relatedly, a justification of why the drag coefficients had to be changed by a factor of 100 should be explored.*
>
> *(19) Plate conditions are difficult to replicate and the rheology of plates likely depends on a number of factors, but is for example, changes in hydration level likely to produce a 100-fold change in drag? or something more interesting/subtle within the model producing the discrepancy?*

18, 19: As mentioned in the paper, we do not know if the friction coefficients in the study of Boyle et al. (2012) and the friction coefficients in the experiment of Stephens et al. (2016) are the same. In our revised manuscript, we have explored more in detail the effects of the friction coefficient's scale factor, and explained why we chose a scale factor of 1/100 (“Proper Selection of Friction Coefficients” in Supplementary Information). In summary, we analyzed the changes in trajectory due to scaling of the friction coefficient, and chose the scale factor 1/100 as it allowed ElegansBot to accurately reproduce the worm's trajectory while also being close to the friction coefficients in the Boyle et al. paper.

> *(20) Finally, the language used to distinguish different modeling approaches was often unclear.*
>
> *(21) For example, it was unclear in what sense the model presented in Boyle, 2012 was a "kinetic model" and in many situations, it appeared that the term kinematic might have been more appropriate. Thank you for the feedback. As you pointed it out, we have corrected that part to 'kinematic' in the revised manuscript.*
>
> *(22) Other phrases like "frictional forces caused by the tension of its muscles" were unclear at first glance, and might benefit from revision and more canonical usage of terms.*

We agree that the expression may not be immediately clear. This is due to the word limit for the abstract (the abstract of eLife VOR should be under 200 words, and our paper's abstract is 198 words), which forced us to convey the causality in a limited number of words. Therefore, although we will not change the abstract, the expression in question means that the muscle tension, which is the cause of the worm's locomotion, ultimately generates the frictional force between the worm and the ground surface.

> ***Recommendations For The Authors***
>
> *(23) As I stated in my public review, I think the paper could be made much stronger if a more detailed exploration of turning mechanics was presented.*
>
> *(24) Relatedly, rather than restricting the analysis to individual videos of turning behaviors, I wonder if a parameterized model of the turning kinematics would be fruitful to study, to try to understand how different turning gaits might be more or less energetically favorable.*

We thank the reviewer once again for their suggestion. Thanks to their proposal, we were able to conduct additional quantitative analysis on turning behavior.

> ***Reviewer #2***
>
> ***Public Review***
>
> *Summary:*
>
> *(1) Developing a mechanical model of C. elegans is difficult to do from basic principles because it moves at a low (but not very small) Reynolds number, is itself visco-elastic, and often is measured moving at a solid/liquid interface.*
>
> *(2) The EleganSBot is a good first step at a kinetic model that reproduces a wide range of C. elegans motiliy behavior.*
>
> *Strengths: (3) The model is general due to its simplicity and likely useful for various undulatory movements.*
>
> *(4) The model reproduces experimental movement data using realistic physical parameters (e.g. drags, forces, etc).*
>
> *(5) The model is predictive (semi?) as shown in the liquid-to-solid gait transition.*
>
> *(6) The model is straightforward in implementation and so likely is adaptable to modification and addition of control circuits.*
>
> *Weaknesses:*
>
> *(7) Since the inputs to the model are the actual shape changes in time, parameterized as angles (or curvature), the ability of the model to reproduce a realistic facsimile of C. elegans motion is not really a huge surprise. (8) The authors do not include some important physical parameters in the model and should explain in the text these assumptions.*
>
> *(9. 1) The cuticle stiffness is significant and has been measured [1].*
>
> *(10. 2) The body of C. elegans is under high hydrostatic pressure which adds an additional stiffness [2].*
>
> *(11. 3) The visco-elasticity of C. elegans body has been measured. [3]*

Thank you for asking. The stiffness of C. elegans is an important consideration. We took this into account when creating EleganSBot, but did not explain it in the paper. The detailed explanation is as follows. C. elegans indeed has stiffness due to its cuticle and internal pressure. This stiffness is treated as a passive elastic force (elastic force term of lateral passive body force) in the paper of Boyle et al. (2012). However, the maximum spring constant of the passive elastic force is 1/20 of the maximum spring constant of the active elastic force. If we consider this fact in our model, the elastic term of the muscle torque (τ_κ) is as follows: (κ_1 is the active torque elasticity coefficient, κ_2 is the passive torque elasticity coefficient)

$$\tau_\kappa = \kappa_1(\theta - \theta_{\text{ctrl}}) + \kappa_2(\theta - 0) = (\kappa_1 + \kappa_2)\left(\theta - \frac{\kappa_1}{\kappa_1+\kappa_2}\theta_{\text{ctrl}}\right) = \kappa\left(\theta - \tilde{\theta}_{\text{ctrl}}\right)$$

where $\kappa \equiv \kappa_1 + \kappa_2$ and $\tilde{\theta}_{\text{ctrl}} \equiv \frac{\kappa_1}{\kappa_1+\kappa_2}\theta_{\text{ctrl}}$

Therefore, there is no need to describe the active and passive terms separately in τ_κ.

Furthermore, since $\kappa_2 = \frac{\kappa_1}{20}$, assuming $\kappa \simeq \kappa_1$,, then $\tilde{\theta}_{\text{ctrl}} \simeq \theta_{\text{ctrl}}$ and $\tau_\kappa \simeq \kappa(\theta - \theta_{\text{ctrl}})$..

> *(12) There is only a very brief mention of proprioception.*
>
> *(13) The lack of inclusion of proprioception in the model should be mentioned and referenced in more detail in my opinion.*

As you emphasized, proprioception is an important aspect in the study of C. elegans' locomotion. In our paper, its importance is briefly introduced with a sentence each in the introduction and discussion. However, our research is a model about the process of the creation of body motion originated from muscle forces, and it does not model the sensory system that senses body posture. Therefore, there is no mention of using proprioception in our paper's results section. What is mentioned in the discussion is that EleganSBot can be applied as the kinetic body model part in a combination model of a kinetic body model and a neuronal circuit model that receives proprioception as a sensory signal.

> *(14) These are just suggested references.*
>
> *(15) There may be more relevant ones available.*

The papers you provided contain specific information about the Young's modulus of the C. elegans body. The first paper (Rahimi et al., 2022) measured the Young's modulus of the cuticle after chemically isolating it from C. elegans, while the second paper (Park et al., 2007) and third paper (Backholm et al., 2013) measured the elasticity and Young's modulus of C. elegans without separating the cuticle. Based on the Young's modulus provided in each paper (although the second and third papers did not measure stiffness in the longitudinal direction), we derived the elastic coefficient (assuming a worm radius of 25 μm, cuticle thickness of 0.5 μm, and 1/25 of longitudinal length of the cuticle of 40 μm). The range was quite broad, from 9.82x1011 μg/sec2 (from the first paper) to 2.16 x 108 μg / sec2 (from the third paper). Although the elastic coefficient value in our paper falls within this range, since the range of the elastic coefficient is wide, we think we can modify the elastic coefficient in our paper and will be able to reapply our model if more accurate values become known in the future.

> ***Reviewer #3***
>
> ***Public Review***
>
> *Summary:*
>
> *(1) A mechanical model is used with input force patterns to generate output curvature patterns, corresponding to a number of different locomotion behaviors in C. elegans*

> *Strengths:*
>
> *(2) The use of a mechanical model to study a variety of locomotor sequences and the grounding in empirical data are strengths.*
>
> *(3) The matching of speeds (though qualitative and shown only on agar) is a strength.*
>
> *Weaknesses:*
>
> *(4) What is the relation between input and output data?*

ElegansBot takes the worm's body control angle as the input, and produces trajectory and force of each segment of the worm as the output.

> *(5) How does the input-output relation depend on the parameters of the model?*

If 'parameter' is understood as vertical and horizontal friction coefficients, then the explanation for this can be found in Fig. 5 (Fig. 4 in the old version).

> *(6) What biological questions are addressed and can significant model predictions be made?*

Equation of motion deciphering locomotion of C. elegans including turning behaviors which were relatively less well understood.

> ***Recommendations For The Authors***
>
> *(7) The novelty and significance of the paper should be clarified.*

We have added quantitative analyses of turning behavior in the revised manuscript, and we hope this will be helpful to you.

> *(8) Previously much more detailed models have been published, as compared to this one.*

We hope the reviewer can point out any previous model that we may have missed.

> *(9) The mechanics here are simplified (e.g. no information about dorsal/ventral innervation but only a bending angle) setting limitations on the capacity for model predictiveness.*
>
> *(10) Such limitations should be discussed.*

We view the difference between dorsal/ventral innervation and bending angle not as a matter of simplification, but rather as a reflection of the hierarchy that our model implements. Our model does not consider dorsal/ventral innervation, but it uses the bending angle to reproduce behavior in various input and frictional environments, which signifies the strong predictiveness of ElegansBot (Figure 2, 3, 5 (2, 3, 4 in the old version)). Moreover, if the midline of C. elegans is incompressible, then modeling by dividing into dorsal/ventral, as opposed to modeling solely with the bending angle, does not increase the degree of freedom of the worm model, and therefore does not increase its predictiveness.

> *(11) The aims of the paper and results need to be supported quantitatively and analyzed through parameter sweeps and intervention.*

We have conducted additional quantitative analyses on turning behavior as suggested by Reviewer #1 (Fig. 4, S4-S7, S9, and S10).

> *(12) The methods are given only in broad brushstrokes, and need to be much more clear (and ideally sharing all code).*

We have thoroughly detailed every aspect of this research, from deriving the physical constants of C. elegans, agar, and water to developing the formulas and proofs necessary for operating EleganSBot and its applications. This comprehensive information is all presented in the Results, Methods, and Supplementary Information sections, as well as in the source code. Moreover, we have already ensured that our research can be easily reproduced by providing detailed explanations and by making EleganSBot accessible through public software databases (PyPI, GitHub). To further aid in its application and understanding, especially for those less familiar with the subject, we have also included minimal code as examples in the database. This code is designed to simplify the process of reproducing the results of the paper, thereby making our research more accessible and understandable. Therefore, we believe that readers will easily gain significant assistance from the extensive information we have provided. Should readers require further help, they can always contact us, and we will be readily available to offer support.

> *(13) The supporting figures and movies need to include a detailed analysis to evidence the claims.*

We have conducted and provided additional quantitative analyses on turning behavior as suggested by Reviewer #1 (Fig. 4, S4-S7, S9, and S10).